Open Access Full Text Article

ORIGINAL RESEARCH

LncRNA PTS-1 Protects Against Osteoarthritis Through the miR-8085/E2F2 Axis

Cheng Ma [1],*, Qi Chen[2],*, Yi-Fan Wei[1],*, Shu-Wen Chen[3], Huan Liu[4], Feng Xin[5], Yong-Xin Ren [1]

[1]Department of Orthopaedics, The First Affiliated Hospital of Nanjing Medical University, Nanjing, Jiangsu, People's Republic of China; [2]Department of Orthopaedics, The Affiliated Changzhou No.2 People's Hospital of Nanjing Medical University, Changzhou, Jiangsu, People's Republic of China; [3]Department of Clinical College, The First Clinical School of Nanjing Medical University, Nanjing, Jiangsu, People's Republic of China; [4]Department of Orthopaedics, The Affiliated Huai'an No.1 People's Hospital of Nanjing Medical University, Huai'an, Jiangsu, People's Republic of China; [5]Department of Orthopaedics, Xuzhou Cancer Hospital, Xuzhou, Jiangsu, 221005, People's Republic of China

*These authors contributed equally to this work

Correspondence: Feng Xin; Yong-Xin Ren, Email 925866554@qq.com; renyongxinjsph@163.com

Background: Osteoarthritis (OA) is a leading cause of pain, disability, and reduced mobility worldwide, characterized by metabolic imbalances in chondrocytes, extracellular matrix (ECM), and subchondral bone. Emerging evidence highlights the critical role of long non-coding RNAs (lncRNAs) in OA pathogenesis. This study focuses on lncRNA PTS-1, a novel lncRNA, to explore its function and regulatory mechanisms in OA progression.
Methods: The expression profile of lncRNAs was assessed using RNA sequencing and qRT-PCR. The expression of lnc-PTS-1 was further validated by qRT-PCR in degenerated cartilage tissues, degenerative primary chondrocytes, and IL-1β-treated C28/I2 cells. Cell viability, proliferation, and apoptosis rates, along with the mRNA and protein levels of apoptosis-related markers (cleaved Caspase 3, cleaved Caspase 9, Bcl-2, Bax), ECM metabolism markers (MMP-3, MMP-13, aggrecan, collagen II), and inflammation-related markers (IL-1β, IL-6, TNF-α) were evaluated using Cell Counting Kit-8, Toluidine Blue staining, Alcian Blue staining, flow cytometry, qRT-PCR, immunofluorescence, and Western Blot. The interaction between miR-8085 and lnc-PTS-1 or E2F2 was investigated through dual luciferase reporter assays and RNA immunoprecipitation (RIP) analyses.
Results: Lnc-PTS-1 expression was significantly downregulated in degenerated cartilage tissues, IL-1β-induced degenerative primary chondrocytes and C28/I2 cells. Functional experiments showed that lnc-PTS-1 knockdown aggravated IL-1β-induced ECM degradation, chondrocyte apoptosis, and inflammation, while its overexpression provided protective effects. Mechanistically, lnc-PTS-1 acted as a competing endogenous RNA (ceRNA) by sponging miR-8085, thereby upregulating E2F2 expression. Notably, miR-8085 upregulation diminished the protective effects of lnc-PTS-1 on ECM degradation, apoptosis, and inflammation, while E2F2 upregulation partially alleviated IL-1β-induced damage. However, these mitigating effects were reversed by miR-8085 overexpression.
Conclusion: These findings identify lnc-PTS-1/miR-8085/E2F2 axis as a novel regulatory mechanism in OA pathogenesis, providing theoretical basis and experimental evidence for the potential clinical application of new lncRNA molecules in the treatment of OA.
Keywords: osteoarthritis, long non-coding RNA PTS-1, E2F2, miR-8085

Introduction

Osteoarthritis (OA) is a prevalent and debilitating joint disorder, particularly among the aging population, affecting over 500 million people worldwide.[1] The disease's complexity is reflected in its multifactorial etiology, involving genetic predisposition, age, obesity, and biomechanical stress.[2,3] Traditionally viewed as a "wear and tear" disease, OA is now recognized as involving more intricate molecular and cellular mechanisms, including inflammation and dysregulated signaling pathways.[4,5] A key aspect of OA progression is the degradation of articular cartilage, driven by chondrocyte apoptosis and extracellular matrix (ECM) breakdown, which leads to joint dysfunction and pain.[6,7] Despite various therapeutic approaches, such as Nonsteroidal Anti-inflammatory Drugs (NSAIDs) and surgical interventions, effective treatments that target the underlying molecular mechanisms of OA are still lacking.[8,9]

Long non-coding RNAs (lncRNAs) have emerged as significant regulators in various biological processes, including OA. LncRNAs are RNA molecules longer than 200 nucleotides that do not encode proteins. Initially considered transcriptional "noise", lncRNAs have now been recognized for their crucial roles in transcriptional regulation, epigenetic modification, RNA stability, and protein translation.[10] Unlike mRNAs, which are broadly conserved and expressed across tissues, lncRNAs often display high tissue specificity and are implicated in fine-tuning cellular functions in specific biological contexts.[11–13] This tissue-specific expression suggests that lncRNAs may play important roles in the cellular processes underlying OA progression.

In OA, lncRNAs have been found to regulate chondrocyte function and ECM homeostasis.[14] Chondrocytes, the primary cell type in articular cartilage, are responsible for maintaining the balance between ECM synthesis and degradation.[15] In OA, this balance is disrupted, leading to cartilage degradation. Recent studies have identified several lncRNAs that modulate chondrocyte proliferation, apoptosis, and the expression of catabolic enzymes.[16,17] For example, LncRNA FOXD2-AS1 suppresses miR-206, leading to upregulation of CCND1 and promoting chondrocyte proliferation, which may counteract cartilage degradation.[18] Similarly, LncRNA PVT1 targets miR-149 to promote apoptosis and ECM degradation, highlighting its potential role in OA pathology.[19] These findings underscore the critical role of lncRNAs in regulating key molecular pathways involved in OA.

LncRNAs also play a significant role in modulating inflammatory responses in the joint microenvironment, a key driver of OA progression. Inflammatory cytokines such as IL-1β and TNF-α are known to exacerbate cartilage degradation by upregulating matrix metalloproteinases (MMPs) and ADAMTS enzymes, which are pivotal in ECM breakdown.[20,21] lncRNAs can influence these inflammatory pathways through various mechanisms, including acting as competing endogenous RNAs (ceRNAs) that modulate miRNA activity or directly interacting with key signaling molecules.[22,23] For instance, LncRNA ANCR promotes chondrocyte proliferation and is inversely correlated with TGF-β1 expression, suggesting it may help mitigate inflammation-induced cartilage damage.[24]

Given their diverse roles in OA, lncRNAs represent promising therapeutic targets. Modulating specific lncRNAs could potentially regulate the expression of genes involved in chondrocyte survival, ECM maintenance, and inflammatory responses, providing a more targeted approach to OA therapy. In this study, we utilized RNA sequencing and qRT-PCR to identify and characterize lnc-PTS-1, whose expression is notably downregulated in human OA tissue and degenerative chondrocyte. Further research is essential to fully elucidate its underlying mechanism.

MicroRNAs (miRNAs) are small, non-coding RNA molecules, typically 20–22 nucleotides in length, that regulate gene expression by binding to complementary sequences in the 3' untranslated regions (UTRs) of target messenger RNAs (mRNAs), leading to mRNA degradation or translation inhibition.[25] In OA, miRNAs regulate various cellular processes, such as chondrocyte proliferation, apoptosis, ECM homeostasis, and the expression of catabolic enzymes.[26] In this context, we identified miR-8085 as a downstream target of lnc-PTS-1 in OA. MiR-8085 has been identified as differentially expressed in osteoporosis cases without fractures compared to controls, highlighting it as a potential therapeutic target in these conditions.[27] However, the role of miR-8085 in OA metastasis and the underlying regulatory mechanisms between lnc-PTS-1 and miR-8085 remain to be fully elucidated.

E2F2 is a member of the E2F family of transcription factors, which regulate cell cycle progression and DNA synthesis, particularly during the transition from the G1 phase to the S phase.[28] Dysregulation of E2F2 has been linked to cancer progression, making it a potential target for cancer therapies aimed at controlling cell proliferation and enhancing DNA damage sensitivity.[29] It has been reported that E2F2-STAT1/MyD88-Akt axis is closely related with the inflammatory phenotype in rheumatoid arthritis synovial fibroblasts.[30]

In this study, we explored the involvement of lncRNAs in OA pathogenesis and tried to decipher the mechanism underlying their function. We identified and characterized lncRNAs implicated in OA by analyzing transcriptomic profiles from cartilage tissues of OA patients and non-OA controls using high-throughput sequencing. To explore the bio-function of lnc-PTS-1 in OA, we performed loss-of- and gain-of-function experiments in C28/I2 human Chondrocyte cell line. Our results suggested that lnc-PTS-1 acts as a ceRNA by "sponge binding" miR-8085, thereby indirectly regulating the expression of E2F2. We propose lnc-PTS-1/miR-8085/E2F2 axis as a theoretical foundation for potential therapeutic targeting of OA. These findings could contribute to improved early diagnosis, treatment strategies, and prognosis of OA, ultimately enhancing patient outcomes.

Materials and Methods

Patients and Tissue Samples Collection

The human cartilage tissue samples were obtained from patients who underwent total hip arthroplasty at the Huai'an No.1 People's Hospital of Nanjing Medical University. These tissues were collected from 10 hip OA patients and 10 femoral neck fracture (FNF) patients without OA (Supplementary Table 1). There is no statistical difference in gender and age between the included patients with FNF and those with hip OA (Supplementary Table 2). All the tissues were immediately preserved in RNALater™ (Beyotime), placed on ice, and then transferred to liquid nitrogen for storage. This study obtained written informed patient consent and was approved by the ethics committee of Nanjing Medical University (approval number: YX-Z-2022-038-01). All procedures performed in the study were in accordance with the Declaration of Helsinki.

Primary Human Chondrocytes and C28/I2 human Chondrocyte Cell Line Obtained and Culture

The cartilage tissue obtained from femoral neck fracture patients without OA was cut into about 2.0 mm^3 size. After washing three times with phosphate-buffered saline (PBS), serum-free DMEM/F12 of 0.25% trypsin was added, digested in a 5% CO_2 incubator at 37°C for 30 minutes. Next, the tissue was cultured in DMEM/F12 supplemented with 0.2% Collagenase type II, 10% fetal bovine serum (FBS) and 1% Penicillin-Streptomycin for 17~24 h. Cells were filtered through a 200-mesh cell strainer and collected at a rate of 1500 r/min for 5 min. Then remove the supernatant and wash the precipitation by complete culture medium with 10% FBS. Finally, the cells were inoculated in a 10 cm cell culture dish and cultured in a 5% CO_2 incubator at 37°C. The cells in the culture dish were fused to about 80% to 90%, and the ratio of 1:2 was passed for subsequent experiments.

C28/I2 human chondrocyte cell line were purchased from the Cell Bank of Type Culture Collection of Chinese Academy of Sciences and used in this study. C28 cells were propagated in DMEM/F12 containing 10% FBS and 1% penicillin-streptomycin in a 37°C, 5% CO_2 incubator. The complete culture medium was replaced every 2~3 days. When the cells were 80% to 90% full, passage was performed with 0.25% trypsin in a ratio of 1:3.

Establishment of Chondrocyte Degeneration Model

The freeze-dried powder of 10 μg IL-1β was dissolved in 100 μL ddH$_2$O and configured as 100 μg/mL storage solution for storage at −80°C for future use. According to the purpose of the experiment, different concentrations of IL-1β (0, 1, 5, 10 ng/mL) were added into cell culture plates, and various experimental methods were used to verify whether the chondrocyte degeneration model was successfully established.

Cell Transfection

Lnc-PTS-1 siRNA/siRNA-negative control (NC), miR-8085 mimics/mimics-NC and their inhibitors/inhibitor-NC were synthesised and purified by Rib Bio (Guangzhou, China). Plasmids containing lnc-PTS-1 expression gene or E2F2 expression gene and control vector plasmids were produced by GeneChem (Shanghai, China). C28/I2 cells were seeded in 6-well plates according to 2×10^5 cells per well, gently pipetted up and down to mix the cells until evenly and put in the incubator overnight. Cell transfection was performed 12~24 hours later when the cells were fully adherent and in good condition by microscopy. Si-RNAs/Si-NC, miRNA-mimics/mimics-NC, miRNA-inhibitor/inhibitor-NC or Plasmids were transfected into C28/I2 cells using Lipofectamine 3000 or X-treme GENE HP DNA Transfection Reagent in OPTI-MEM medium. After 6 hours of transfection, cells were changed to complete medium and then cultured for another 24~48 hours. Finally, C28/I2 cells were collected for RNA or protein extraction or subjected to immunofluorescence staining.

Cell Viability Assessment

Cell viability was assessed using Cell Counting Kit-8 (CK05, DOJINDO, China). The C28/I2 cells with different treatment were cultured in a 96-well multiplate at 5×10^3 cells per well, followed by incubation with a complete culture

medium for 24, 48, and 72 hour after cell attachment. Cell Counting Kit-8 (CCK-8) assays were applied to measure the absorbance at the 24-, 48-, and 72-hour time points using SpectraMaxM (Molecular Devices, Shanghai, China), according to the manufacturer's instructions.

Cell Staining

The C28/I2 cells with different treatment were cultured in a 6-well plates at 2×10^5 cells per well, then stained as follows. The Toluidine Blue staining (G3660, Solarbio, China) and Alcian Blue (G1565, Solarbio, China) were used in accordance with the manufacturer's instructions. For Toluidine Blue staining, chondrocytes were fixed with 4% paraformaldehyde, stained with toluidine blue for 2 hours, washed with PBS, and mounted with neutral medium for microscopic analysis. For Alcian Blue staining, chondrocytes were fixed with 4% paraformaldehyde, washed with PBS, treated with Alcian acid solution for 3 minutes, and stained with Alcian staining solution for 30 minutes, washed with PBS, and mounted with neutral medium for microscopic analysis. The immunofluorescence (IF) assay was performed as previously described.[31] Chondrocytes were seeded into 24-well plates, induced with IL-1β to model degeneration, and transfected according to the experimental design. Cells were fixed with 4% paraformaldehyde, permeabilized with 0.5% Triton X-100-5% BSA-PBS, and blocked with 5% BSA-PBS. Primary antibodies were applied overnight at 4°C, followed by washing and incubation with fluorescent secondary antibodies for 60 minutes in the dark. Coverslips were mounted with DAPI on slides. All specific antibodies involved in IF staining are listed in Supplementary Table 4. Images were acquired using the Leica DMi8 fluorescent microscope with the Leica LAS-X software and analyzed with the ImageJ software (NIH).

RNA Isolation, Analysis and Primer Sequences

Total RNAs were isolated from human cartilage tissue and cultured C28/I2 cells using the Trizol reagent (Invitrogen) and reverse transcribed into complementary DNA by the HiScript III RT SuperMix for quantitative PCR (qPCR; R302-01, Vazyme, Nanjing, China). The relative levels of mRNA normalized to GAPDH and miRNA normalized to U48 expression were calculated using comparative $2^{-\Delta\Delta CT}$ method. Operate and analyze according to the procedures described in the previously published article.[31] Supplementary Table 3 presents the qRT-PCR primer sequences.

Western Blot and Antibodies

Western Blot was performed to analyze the protein expression of ECM anabolism related-, apoptotic related-, and inflammation related-markers, according to the procedure described in a previously published article.[32] Equal amounts of protein samples were separated by sodium dodecyl sulfate-polyacrylamide gel electrophoresis gels and transferred to polyvinylidene difluoride (PVDF) membranes. After blocking with 5% skim milk solution for one hour, the membrane was incubated overnight with different primary antibodies at 4°C. Then, membrane incubation with secondary antibody matched to primary antibody. Bands were visualized by the ECL Western Blot assay kit and analyzed by ImageJ software. The list of primary and secondary antibodies is shown in Supplementary Table 4.

Flow Cytometric Analysis

Flow cytometry analysis was performed to analyze apoptosis levels by using FITC Annexin V Apoptosis Detection Kits (C1062M, Beyotime, China). Cells were cultured and transfected as described. After 48 hours, the medium was transferred to a flow cytometry tube, and cells were washed with PBS. Cells were treated with trypsin, stopped with the collected medium, detached, and centrifuged at 1000 rpm for 5 minutes. After discarding the supernatant, cells were washed twice with PBS and resuspended in Annexin V-FITC binding buffer. Annexin V-FITC and propidium iodide were added, mixed, and incubated in the dark for 20 minutes. Apoptotic cells were determined using Flow cytometer (BD Technologies) and analyzed with FlowJo.

RNA Nuclear and Cytoplasmic Isolation Analysis

RNA nuclear and cytoplasmic isolation analysis was performed according to the manufacturer's instructions of the PARIS™ Kit (AM1921, Life). Briefly, cells were washed with ice-cold PBS, lysed with Cell Disruption Buffer on ice, and centrifuged at 500 × g for 5 minutes at 4°C to separate the nuclear and cytoplasmic fractions. The cytoplasmic supernatant was transferred to a new tube, while the nuclear pellet was resuspended in Cell Disruption

Buffer. RNA was isolated from both fractions using the kit's RNA extraction reagents. Purified RNA was quantified and assessed for quality using a spectrophotometer. Reverse transcription and quantitative PCR were performed on the isolated RNA using the methods described above.

RNA Immunoprecipitation (RIP) Assays

RIP experiments were performed to investigate the relationship between miR-8085 and lncRNA lnc-PTS-1 or E2F2 using a Magna RIPTM RNA-Binding Protein Immunoprecipitation Kit (Cat. 17–701, Millipore, USA), according to the manufacturer's instructions. C28/I2 chondrocytes were cultured to 80–90% confluence, digested, and resuspended in PBS. Cells were centrifuged at 1000 × g for 5 minutes, and the pellet was lysed using RNA Immunoprecipitation Kit lysis buffer. Magnetic beads pre-incubated with Argonaute2 or IgG antibodies were added to the lysate to capture the Argonaute2-RNA complex. After washing, RNA was extracted, reverse-transcribed, and analyzed by qRT-PCR, followed by statistical analysis.

Dual Luciferase Assay

Dual luciferase Assay was performed to investigate the relationship between miR-8085 and lncRNA lnc-PTS-1 or E2F2. HEK 293T cells were seeded in 24-well plates, and the cells were allowed to adhere to the wall overnight. Then, the cells were transfected with lnc-PTS-1 wild-type 3′UTR/mutant 3′UTR or E2F2 wild-type 3′UTR/mutant 3′UTR luciferase reporter vector and mimic-NC, miR-8085 mimic, inhibitor-NC, or miR-8085 inhibitor by using Lipofectamine 3000 (Invitrogen). After 36h transfection, Dual Luciferase Reporter Gene Assay Kit (YEASEN, 11402ES60) was used to measure the luciferase activity.

Statistical Analysis

All statistical analyses were performed using GraphPad Prism Version 10.0. The results are shown as mean ± standard deviation (SD). The Student's t-test or one-way analysis of variance (ANOVA) was employed for comparisons between groups. The miRNA differential expression level based on normalized deep-sequencing counts was analyzed by selectively using the Fisher exact test, chi-square 2×2 test, chi-squared N × N test, Student's t-test, or ANOVA. P values < 0.05 were considered statistically significant.

Results

lnc-PTS-1 is Deficient in Human Osteoarthritic Cartilage

To investigate the expression profile of Long Non-Coding RNAs (lncRNAs) in osteoarthritis, we used microarray screening (RNA-seq) on cartilage tissues from osteoarthritis (OA, n=3) or normal patients (Con, n=3). A total of 682 significantly up-regulated lncRNAs and 512 significantly down-regulated lncRNAs were filtered according to $\log_2 FC > 1.5$ or < -1.5 and FDR < 0.05 (Figure 1A). We selected lncRNAs of the remarkable differential expression for validation in human cartilage. qRT-PCR analysis showed that lnc-PTS-1 was significantly down-regulated in osteoarthritic cartilage, which was concordant with RNA-seq results (Figure 1B). As described in the LNCipedia database (https://lncipedia.org/db/transcript/lnc-PTS-1:4), ENST00000529938 is a 1166-bp lncRNA transcribed from chr11:112,290,268–112,292,170 (Figure 1C and D). Various software analyses revealed that lnc-PTS-1 cannot be transcribed into a protein (Figure 1E). qRT-PCR showed lnc-PTS-1 was deficiently expressed in human osteoarthritic cartilage (n=10) and IL-1β stimulated-degenerative primary chondrocytes or C28/I2 chondrocytes (Figure 1F-H).

Therefore, these data indicated a downregulation of lnc-PTS-1, suggesting a potential role in the pathogenesis of OA.

lnc-PTS-1 Contributed to ECM Anabolism, Anti-Apoptotic Effects, and Anti-Inflammatory Responses in Chondrocytes

To construct a chondrocyte degeneration model, we stimulated C28/I2 chondrocytes with different concentrations of IL-1β. CCK-8 assay showed a decline in cell viability with 5 ng/mL and 10 ng/mL at 24h, 48h and 72h (Supplementary Figure A). Alcian blue staining and Toluidine blue staining indicated IL-1β induced ECM degradation in a concentration dependent
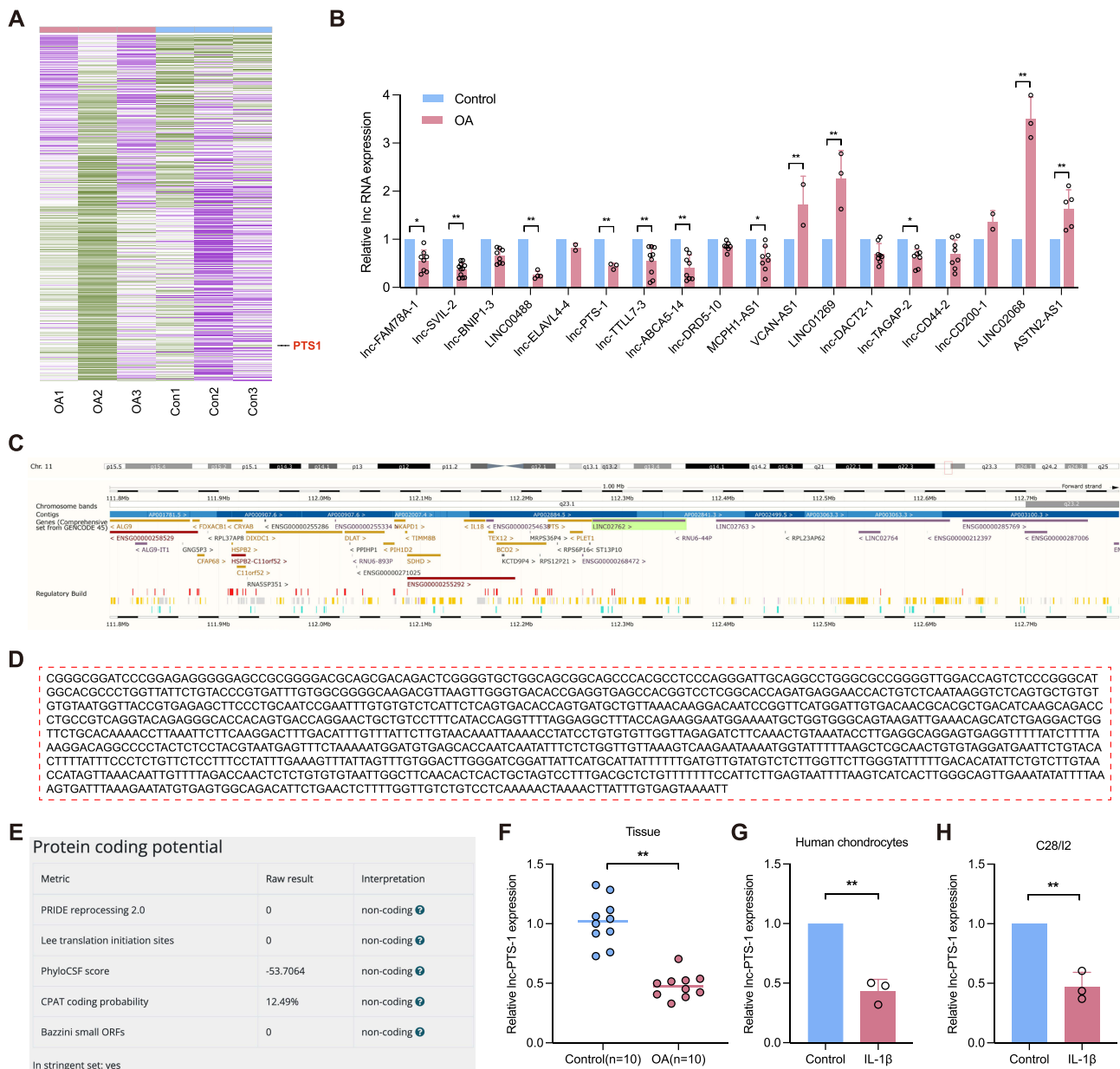
Figure 1 Relative expression and basic characteristics of LncRNA PTS-1 in human cartilage. (**A**) The heatmap of LncRNAs expression profiles between patients of osteoarthritis (OA) group and normal control (Con) group. (**B**) qRT-PCR analysis of the LncRNAs expression of cartilage tissue from OA patients or normal control. (**C**) NCBI database indicated the chromosomal localization of lnc-PTS-1. (**D**) The full sequence of lnc-PTS-1, as excerpted from the LNCipedia database. (**E**) The protein coding potential of lnc-PTS-1 as analyzed by different algorithms. (**F–H**) qRT-PCR analysis of lnc-PTS-1 expression of cartilage tissue from OA patients or normal control, degenerative human primary chondrocytes and C28/I2 cells induced by IL-1β. Data are presented as mean ± SD, Statistical analysis was performed using unpaired t-tests; *$P < 0.05$, **$P < 0.01$.

manner (Supplementary Figure B). As shown in Supplementary Figure C-F, 5 ng/mL and 10 ng/mL IL-1β markedly reduced the mRNA and protein expression of collagen II and aggrecan (ACAN), whereas increased ECM catabolism indicators. Flow cytometry analysis showed that IL-1β over 5 ng/mL promoted chondrocytes apoptosis (Supplementary Figure G), and Western Blot and immunofluorescence (IF) assay showed the protein expression of pro-apoptotic Bax, as well as cleaved Caspase 3 and 9, were up-regulated (Supplementary Figure H-J). Besides, chondrocytes expressed more inflammatory cytokines, such as TNF-α and IL-6 (Supplementary Figure K-N). Collectively, these results suggested 10 ng/mL IL-1β stimulation model could simulate chondrocytes degeneration in the pathogenesis of OA.

To explore the biological function of lnc-PTS-1 in OA progression, we transfected C28/I2 with lnc-PTS-1 expression plasmid or siRNA to overexpress or knock down lnc-PTS-1 (Figures 2A and 3A). As shown in Figures 2B and 3B, overexpression of lnc-PTS-1 partially increased cell viability of degenerative chondrocytes, whereas knock down of lnc-PTS-1 further decreased cell viability. Alcian blue staining and Toluidine blue staining indicated overexpression lnc-PTS-1 promoted chondrocytes ECM anabolism (Figure 2C), which was in agreement with up-regulation of the mRNA and protein expression of collagen II and aggrecan and down-regulation of MMP-3, MMP-13, ADAMTS-4 and ADAMTS-5 (Figure 2D-G). lnc-PTS-1 alleviated chondrocytes apoptosis by flow cytometry analysis (Figure 2H) and increased the expression of anti-apoptotic Bcl-2 and decreased Bax, cleaved Caspase-3 and cleaved Caspase-9 (Figure 2I-K). Additionally, lnc-PTS-1 overexpression could remarkably reduce inflammatory factors (Figure 2L-O). By contrast, lnc-PTS-1 knock down exhibited the opposite effects and deteriorated ECM degradation, cell apoptosis and inflammation induced by IL-1β (Figure 3C-O).

Taken together, these data revealed that lnc-PTS-1 attenuated OA progression via stabilizing ECM anabolism, inhibiting apoptosis and inflammation in vitro.

lnc-PTS-1 Physically Interacted with miR-8085 in the Cytoplasm

The biological mechanism of lncRNAs is closely related to its localization. lnc-PTS-1 was found to be distributed in both the cytoplasm and the nucleus, but was more abundant in the cytoplasm with or without IL-1β as demonstrated by RNA nuclear and cytoplasmic separation experiments and fluorescence in situ hybridization (FISH) assay (Figure 4A and B). To screen for miRNAs that physically bind to lnc-PTS-1, miRNA sequence (miRNA-seq) was performed to detect miRNA expression profiles of lnc-PTS-1 knockdown C28/I2 (KD, n=3) and negative control (Con, n=3). A total of 63 significantly up-regulated miRNAs and 21 significantly down-regulated miRNAs were filtered according to $\log_2 FC > 1.0$ or < -1.0 and FDR < 0.05 (Figure 4C and D). According to bioinformatics predictions (RNAhybrid and Miranda) and miRNA-seq results, we expected that lnc-PTS-1 may bind hsa-miR-4758-3p, hsa-miR-5571-3p, hsa-miR-8085, hsa-miR-6752-3p and hsa-miR-6880-5p (Figure 4E).

Then, RNA Binding Protein Immunoprecipitation (RIP) was administrated to confirm the interaction between lnc-PTS-1 and these miRNAs. The result of qRT-PCR showed that compared to anti-IgG group, miR-4758, miR-8085 and lnc-PTS-1 were bound to Ago2 (Figure 4F). Since miR-8085 was the most highly enriched, we selected miR-8085 as a potential candidate interacting with lnc-PTS-1 to further experiments. In the light of the Tarbase predicted that there were two potential binding sites of lnc-PTS-1 and miR-8085 (Figure 4G), we constructed lnc-PTS-1 plasmid (WT) or mutant plasmid (MUT) to implement luciferase reporter assay, which were co-transfected into 293T cells with hsa-miR-8085-mimics, hsa-miR-8085-inhibitor, or negative control, respectively (Figure 4H). As shown in Figure 4I, the relative luciferase activity of lnc-PTS-1 WT and hsa-miR-8085-mimics co-transfection was strikingly lower while that of lnc-PTS-1 WT and hsa-miR-8085-inhibitor co-transfection was strikingly increased, compared to their respective negative controls. However, after transfection with lnc-PTS-1 MUT, there was no significant difference in relative luciferase activity between hsa-miR-8085-mimics and hsa-miR-8085-inhibitor compared with negative control (Figure 4I). Meanwhile, miR-8085 expression was up-regulated in the chondrocytes degenerative model in vitro (Figure 4J).

The above results showed that miR-8085 may bind to lnc-PTS-1 in a targeted manner, which participates in the regulation of OA pathogenesis.

lnc-PTS-1 Functioned as a Sponge for miR-8085 to Regulate Chondrocytes Degeneration

To study the biological effects of miR-8085 regulated by lnc-PTS-1 to chondrocytes regression, we elevated miR-8085 expression in C28/I2 via transfection with miR-8085-mimics, and qRT-PCR confirmed the efficiency (Figure 5A). Then, we transfected miR-8085-mimics in lnc-PTS-1 overexpression or control chondrocytes. As shown in Figure 5B, CCK-8 assay resulted in a decline in cell viability with miR-8085-mimics overexpression compared with NC-mimics group. Alcian blue staining and Toluidine blue staining showed that C28/I2 cells of miR-8085-mimics transfection appeared
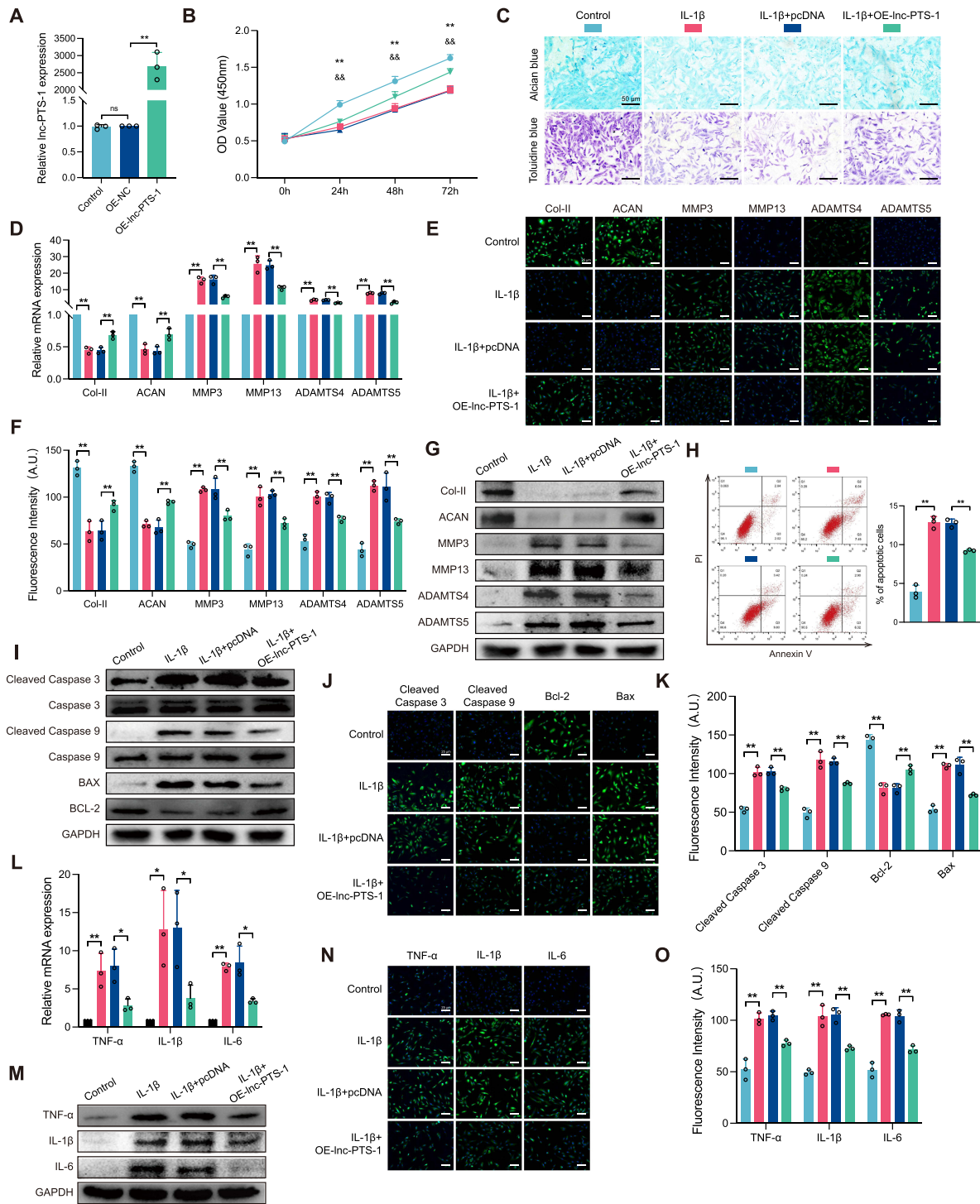
Figure 2 Lnc-PTS-1 contributed to ECM anabolism, anti-apoptotic effects, and anti-inflammatory responses in chondrocytes. (**A**) qRT-PCR analysis of lnc-PTS-1 expression of C28/I2 cells transfected with overexpression plasmid or negative control (n=3). (**B**) CCK-8 assays were performed to determine the cell viability of transfected C28/I2 cells under IL-1β treatment at 24, 48, and 72 h (**$P < 0.01$, Control vs IL-1β; $^{\&\&}P < 0.01$, IL-1β+OE-NC vs IL-1β+OE-lnc-PTS-1) (n=6). (**C**) Alcian blue and Toluidine blue staining (scale bar: 50 μm) were conducted to determine the ECM anabolism of transfected C28/I2 cells under IL-1β treatment (n=3). (**D**) qRT-PCR, (**E** and **F**) representative IF images (scale bar: 25 μm) and quantitative analysis, and (**G**) Western Blot analysis showed expression levels of ECM metabolism indicators of lnc-PTS-1 overexpression C28/I2 cells with IL-1β (n=3). (**H**) The apoptosis rate of C28/I2 cells was showed by flow cytometry (n=3). (**I**) Western Blot analysis, and (**J** and **K**) representative IF images (scale bar: 25 μm) and quantitative analysis showed apoptosis-related indicators expression levels of lnc-PTS-1 overexpression C28/I2 cells with IL-1β (n=3). (**L**) qRT-PCR, (**M**) Western Blot analysis, and (**N** and **O**) representative IF images (scale bar: 25 μm) and quantitative analysis showed expression levels of inflammatory factors of lnc-PTS-1 overexpression C28/I2 cells with IL-1β (n=3). Data are presented as mean ± SD, Statistical analysis was performed using one-way analysis of variance (ANOVA); *$P < 0.05$, **$P < 0.01$, ns, non-significance, $P \geq 0.05$.
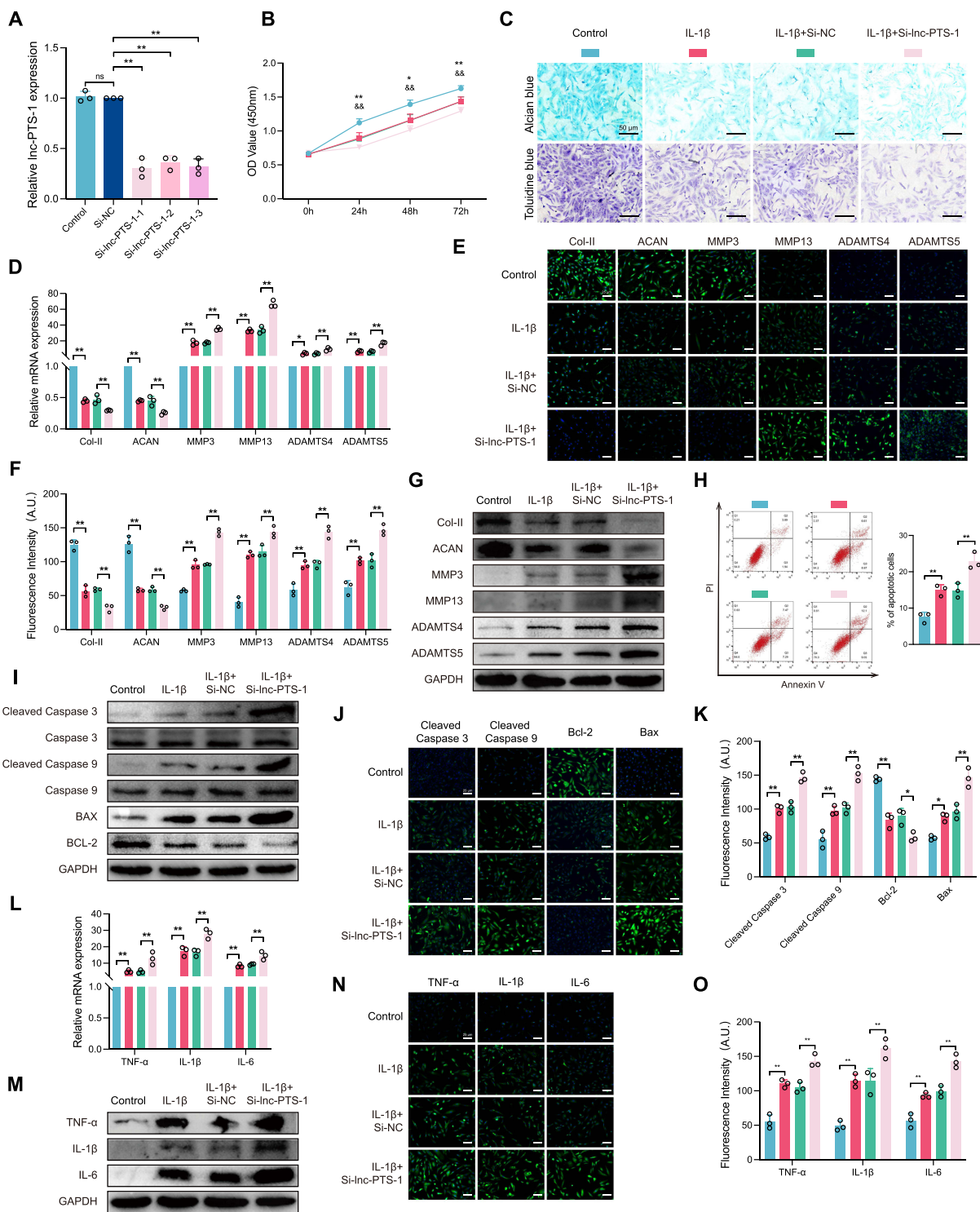
Figure 3 The deficiency of lnc-PTS-1 exacerbated ECM catabolism, apoptosis, and inflammatory responses in chondrocytes. (**A**) qRT-PCR analysis of lnc-PTS-1 expression of C28/I2 cells transfected with siRNAs or negative control (n=3). (**B**) CCK-8 assays were performed to determine the cell viability of transfected C28/I2 cells under IL-1β treatment at 24, 48, and 72 h (*$P < 0.05$, **$P < 0.01$, Control vs IL-1β; &&$P < 0.01$, IL-1β+Si-NC vs IL-1β+Si-lnc-PTS-1) (n=6). (**C**) Alcian blue and Toluidine blue staining (scale bar: 50 μm) were conducted to determine the ECM anabolism of transfected C28/I2 cells under IL-1β treatment (n=3). (**D**) qRT-PCR, (**E** and **F**) representative IF images and quantitative analysis, and (**G**) Western Blot analysis showed expression levels of ECM metabolism indicators of lnc-PTS-1 knock down C28/I2 cells with IL-1β (n=3). (**H**) The apoptosis rate of C28/I2 cells was showed by flow cytometry (n=3). (**I**) Western Blot analysis, and (**J** and **K**) representative IF images (scale bar: 25 μm) and quantitative analysis showed apoptosis-related indicators expression levels of lnc-PTS-1 knock down C28/I2 cells with IL-1β (n=3). (**L**) qRT-PCR, (**M**) Western Blot analysis, and (**N** and **O**) representative IF images (scale bar: 25 μm) and quantitative analysis showed expression levels of inflammatory factors of lnc-PTS-1 knock down C28/I2 cells with IL-1β (n=3). Data are presented as mean ± SD, Statistical analysis was performed using one-way analysis of variance (ANOVA); *$P < 0.05$, **$P < 0.01$, ns, non-significance, $P \geq 0.05$.

Figure 4 Lnc-PTS-1 physically interacted with miR-8085 in the cytoplasm. (**A**) Nuclear and cytoplasmic RNA isolation analysis of the distribution of lnc-PTS-1 in C28/I2 cells with or without IL-1β (n=3). (**B**) The FISH assay was used to detect the localization of lnc-PTS-1 in C28/I2 cells. Nuclei were stained with DAPI. Scale bar: 25 μm. (**C**) The heatmap and (**D**) the volcano plot of significant differentially expressed miRNA between lnc-PTS-1 knockdown and Control group (n=3). (**E**) The Venn diagram displayed lnc-PTS-1 computationally predicted to target miRNAs by different algorithms. (**F**) RIP assays for anti-Ago2 were performed in C28/I2 cells and the coprecipitated RNA was subjected to qRT-PCR for predictive five miRNAs (n=3). (**G**) Tarbase database predicted the potential binding sites of miR-8085 with lnc-PTS-1. (**H**) Schematic diagrams of WT or Mutant lnc-PTS-1 luciferase reporter plasmid. (**I**) The dual luciferase activity of HEK 293T cells co-transfected lnc-PTS-1 WT or Mutant plasmid and miR-8085 mimics or inhibitor (n=3). (**J**) Relative miR-8085 expression levels of C28/I2 cells under IL-1β treatment by qRT-PCR (n=3). Data are presented as mean ± SD, Statistical analysis was performed using unpaired t-tests; **$P < 0.01$, ns, non-significance, $P \geq 0.05$.
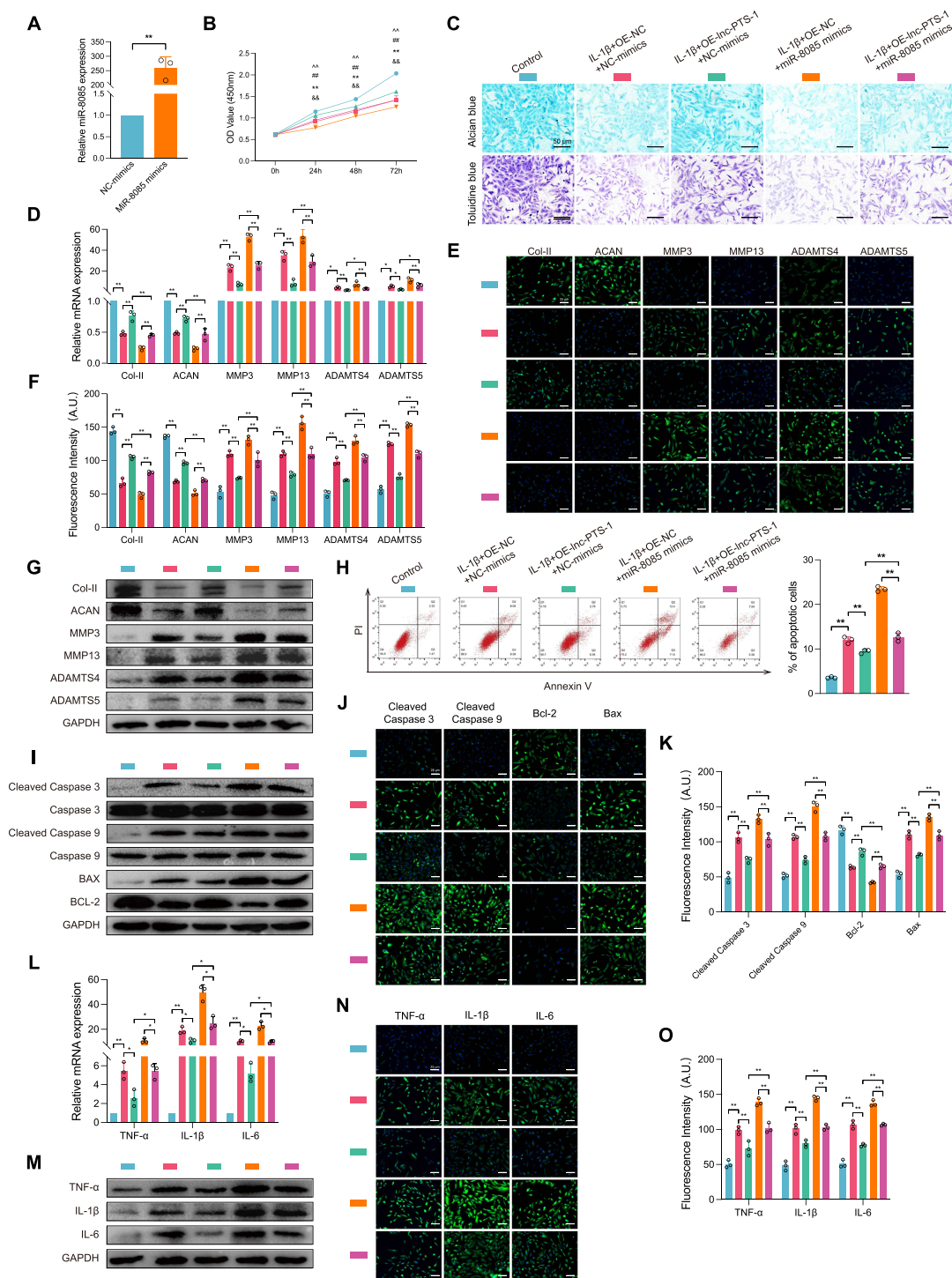
Figure 5 Lnc-PTS-1 functioned as a sponge for miR-8085 to regulate chondrocytes degeneration. (**A**) qRT-PCR analysis of miR-8085 expression of C28/I2 cells transfected with mimics or negative control (n=3). (**B**) CCK-8 assays were performed to determine the cell viability of miR-8085 mimics and lnc-PTS-1 co-transfection with or without IL-1β at 24, 48, and 72 h (**P < 0.01, Control vs IL-1β; &&P < 0.01, IL-1β+OE-NC+NC-mimics vs IL-1β+OE-lnc-PTS-1+NC-mimics, ##P < 0.01, IL-1β+OE-lnc-PTS-1+NC-mimics vs IL-1β+OE-lnc-PTS-1+miR-8085 mimics; ^^P < 0.01, IL-1β+OE-NC+miR-8085 mimics vs IL-1β+OE-lnc-PTS-1+miR-8085 mimics) (n=6). (**C**) Alcian blue and Toluidine blue staining (scale bar: 50 μm) were conducted to determine the ECM anabolism of miR-8085 mimics and lnc-PTS-1 co-transfection with or without IL-1β (n=3). (**D**) qRT-PCR, (**E** and **F**) representative IF images (scale bar: 25 μm) and quantitative analysis, and (**G**) Western Blot analysis showed expression levels of ECM metabolism indicators of miR-8085 mimics and lnc-PTS-1 co-transfected C28/I2 cells with or without IL-1β (n=3). (**H**) The apoptosis rate of C28/I2 cells was showed by flow cytometry (n=3). (**I**) Western Blot analysis, and (**J** and **K**) representative IF images (scale bar: 25 μm) and quantitative analysis showed apoptosis-related indicators expression levels of miR-8085 mimics and lnc-PTS-1 co-transfected C28/I2 cells with or without IL-1β (n=3). (**L**) qRT-PCR, (**M**) Western Blot analysis, and (**N** and **O**) representative IF images (scale bar: 25 μm) and quantitative analysis showed expression levels of inflammatory factors of miR-8085 mimics and lnc-PTS-1 co-transfected C28/I2 cells with or without IL-1β (n=3). Data are presented as mean ± SD, Statistical analysis was performed using unpaired t-tests (**A**) or one-way analysis of variance (ANOVA) (**B, D, F, H, K, L, O**); *P < 0.05, **P < 0.01.

fewer positive staining, suggesting miR-8085 inhibited ECM metabolism, which was in accord with down-regulation of Col-II, ACAN and up-regulation of MMP3, MMP13, ADAMTS4 and ADAMTS5 (Figure 5C-G).

Next, we investigated the role of miR-8055 in the impacts of lnc-PTS-1 on cell apoptosis and inflammation. Flow cytometry analysis showed that miR-8085-mimic increased cell apoptosis ratio compared to NC-mimics (Figure 5H). Western Blot and IF resulted in an elevation of pro-apoptosis indicators and inflammatory cytokines after transfected with miR-8085-mimics, suggesting that miR-8055 overexpression facilitated cell apoptosis and inflammation (Figure 5I-O).

Moreover, comparing to transfection simply with lnc-PTS-1 after IL-1β stimulation, chondrocytes co-transfected with lnc-PTS-1 and miR-8085-mimics deteriorated cell viability decrease, ECM catabolism, apoptosis and inflammation response, which means miR-8085 eliminated a resistance effect induced by lnc-PTS-1 overexpression.

These data suggested that up-regulation of miR-8085 could reverse the effect of exogenous lnc-PTS-1 on ECM anabolism, anti-apoptosis and anti-inflammation in chondrocytes.

RNA-Seq Highlighted lnc-PTS-1 Contributes to Maintaining Chondrocytes Homeostasis

To further validate the impact of lnc-PTS-1 knockdown on the degenerative phenotype of chondrocytes and to explore its underlying molecular mechanisms in greater depth, we performed RNA sequencing (RNA-seq) on lnc-PTS-1 knockdown (KD) and control C28/I2 cells (Con) (n=3 per group). A total of 530 differentially expressed genes (DEGs) exhibited a fold change of over two-fold, with 247 mRNAs being upregulated and 283 mRNAs being downregulated (Figure 6A and B). Our results revealed that lnc-PTS-1 knockdown induces activation of classical chondrocyte degeneration pathways, including hypoxia, DNA damage, and ERK pathway activation (Figure 6C and D). Moreover, protective pathways, such as those involved in DNA replication and cell cycle regulation, were significantly downregulated, while pathways detrimental to cartilage homeostasis, such as apoptosis, ERK pathway activation, and DNA damage, were upregulated following lnc-PTS-1 knockdown (Figure 6D). These findings suggested a protective role of lnc-PTS-1 in maintaining chondrocyte function and cartilage integrity during the progression of osteoarthritis.

MiR-8085 Targeted E2F2 in the Cytoplasm

The potential targets of miR-8085 were predicted by bioinformatics platforms (RNAhybrid, Miranda and Targetscan). An intersection of these predictions with RNA-seq data yielded 7 candidate target mRNA for miR-8085, specifically MEX3B, E2F2, CCDC61, ALX4, MYBL1, TPX2, NEURL1B (Figure 7A). Above-mentioned bioinformatics analysis revealed that lnc-PTS-1 is involved in DNA replication and cell cycle regulation (Figure 6D). Therefore, this study has selected E2F2, a transcription factor involved in cell cycle regulation, as a candidate target gene for miR-8085 to undergo further validation. As depicted in Figure 7B, the RIP assay confirmed that anti-Ago2 co-precipitated with both miR-8085 and E2F2 mRNA, in comparison to anti-IgG group. Targetscan predicted two potential binding sites of E2F2 mRNA for miR-8085 (Figure 7C). Following this, the dual luciferase reporter plasmids were constructed containing the wild-type E2F2 binding site sequence (Luc E2F2 WT) and its mutant sequence (Luc E2F2 MUT) (Figure 7D). These were then transfected into HEK 293T cells, along with co-transfections of hsa-miR-8085-mimics, hsa-miR-8085-inhibitor, and their respective negative controls (NC). The dual luciferase assay demonstrated that the relative luciferase activity of the Luc E2F2 WT group co-transfected with hsa-miR-8085-mimics was significantly lower compared to that co-transfected with NC-mimics (Figure 7E). In contrast, the relative luciferase activity of the Luc E2F2 WT group, where miR-8085 was inhibited, was significantly increased compared to the NC-inhibitor (Figure 7E). Additionally, E2F2 mRNA expression was notably decreased in IL-1β-induced chondrocyte degeneration (Figure 7F). Furthermore, the expression dynamics of lnc-PTS-1 and miR-8085 could influence E2F2 expression. Our study demonstrated that overexpression of lnc-PTS-1 or suppression of miR-8085 resulted in a significant elevation of E2F2 at both the mRNA and protein levels (Figure 7G, 7I-K). Conversely, lnc-PTS-1 knockdown or miR-8085 overexpression led to a marked downregulation of E2F2 (Figure 7H, 7L-N).

Collectively, these findings indicated that miR-8085 binds to E2F2, representing a regulatory mechanism by which lnc-PTS-1 modulates miR-8085 in the progression of chondrocyte degeneration.
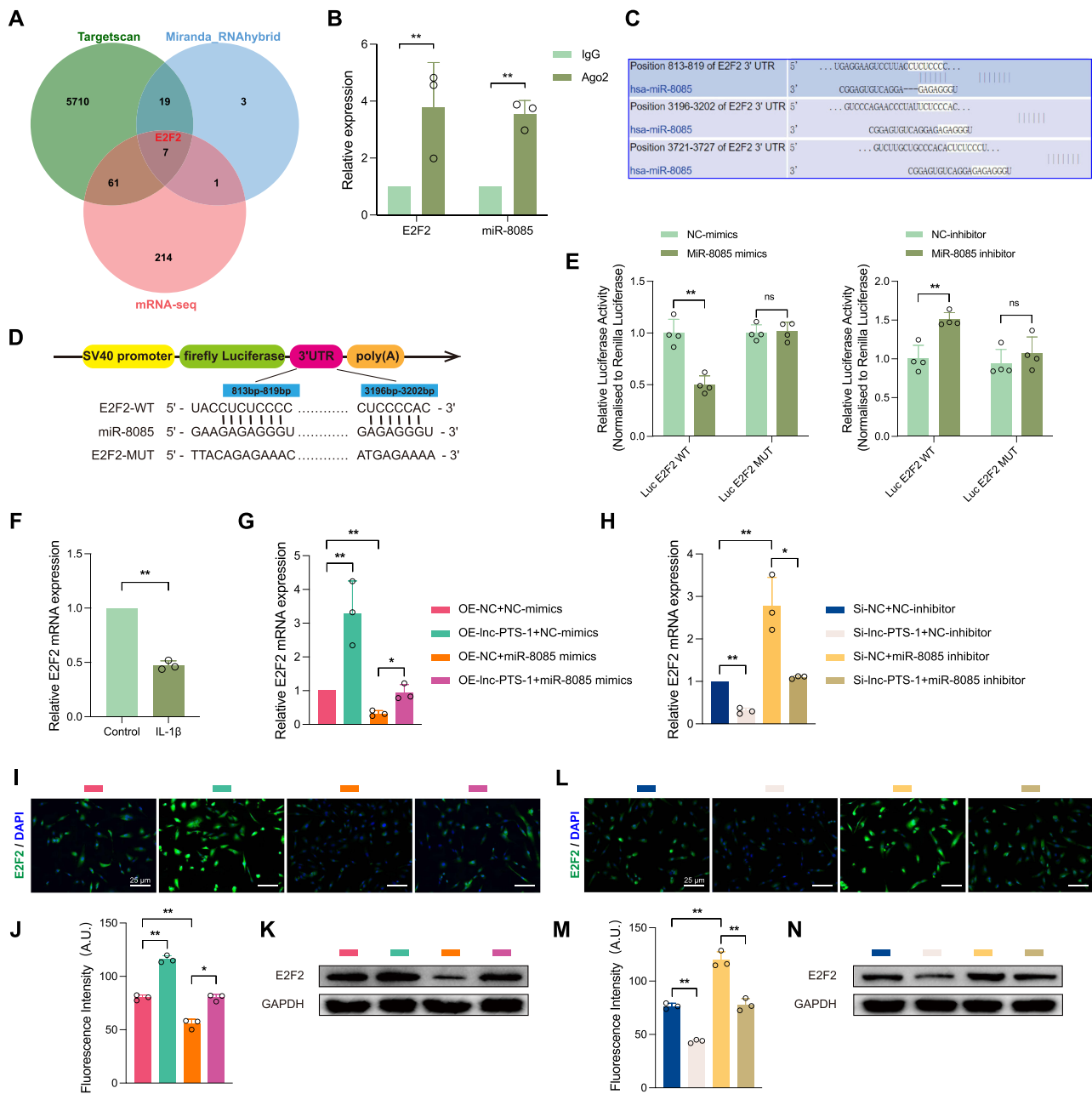
Figure 6 Transcriptomic profiling and bioinformatics analysis of lnc-PTS-1 knockdown or Control. (**A**) The heatmap profiling and (**B**) the volcano plot of transcriptomics in C28/I2 cells between lnc-PTS-1 knockdown (KD) and Control (Con) groups (n=3). (**C**) The bubble charts illustrated the enriched signaling pathways associated with upregulated genes between the KD and Control groups (n=3). (**D**) The concise heatmap showed significant DEGs enriched in signaling pathways between KD group and Control group.

lnc-PTS-1 Regulated the miR-8085/E2F2 Axis to Protect Against OA Progression

To elucidate the regulatory role of miR-8085 on E2F2 in IL-1β-induced chondrocyte degeneration, we established a C28/I2 cell line with E2F2 overexpression. The overexpression efficiency was confirmed by qRT-PCR and Western Blot, as depicted in Figure 8A. CCK-8 assay results indicated that the cell viability of the IL-1β+OE-E2F2-mimics-NC group was significantly higher at various time points compared to the IL-1β+pcDNA+mimics-NC group. In contrast, the cell

Figure 7 MiR-8085 targeted E2F2 in the cytoplasm. (**A**) The Venn diagram compared miR-8085-targeted mRNAs predicted by different algorithms and transcriptomics. (**B**) RIP assays for anti-Ago2 were performed in C28/I2 cells and the coprecipitated RNA was subjected to qRT-PCR for E2F mRNA and miR-8085 (n=3). (**C**) Targetscan database predicted the potential binding sites of miR-8085 and E2F2 mRNA. (**D**) Schematic diagrams of WT or Mutant E2F2 luciferase reporter plasmid. (**E**) The dual luciferase activity of HEK 293T cells co-transfected E2F2 MT or Mutant plasmid and miR-8085 mimics or inhibitor (n=3). (**F**) Relative E2F2 mRNA expression levels of C28/I2 cells under IL-1β treatment by qRT-PCR (n=3). (**G** and **H**) qRT-PCR, (**I, J, L, M**) representative IF images (scale bar: 25 μm), and (**K, N**) Western Blot showed E2F2 expression of miR-8085 mimics or inhibitor and lnc-PTS-1 overexpression or knock down co-transfected C28/I2 cells (n=3). Data are presented as mean ± SD, Statistical analysis was performed using unpaired t-tests (**B, E, F**) or one-way analysis of variance (ANOVA) (**G, H, J, M**); *$P < 0.05$, **$P < 0.01$, ns, non-significance, $P \geq 0.05$.

viability of the IL-1β+OE-E2F2+miR-8085-mimics group was notably reduced when compared to the IL-1β+OE-E2F2 +mimics-NC group (Figure 8B). Alcian Blue and Toluidine Blue staining were employed to assess the expression levels of ECM components. Our findings revealed that chondrocytes overexpressing E2F2 during degeneration exhibited an expanded region of positive staining, however, the co-overexpression of miR-8085 alongside E2F2 resulted in diminished positive staining, suggesting that miR-8085 may counteract the effect of E2F2 overexpression on ECM components (Figure 8C). qRT-PCR, Western Blot, and IF staining were utilized to assess ECM-related indicators expression levels in chondrocytes. In alignment with prior findings, the IL-1β group exhibited a notable decrease in the expression of Col II
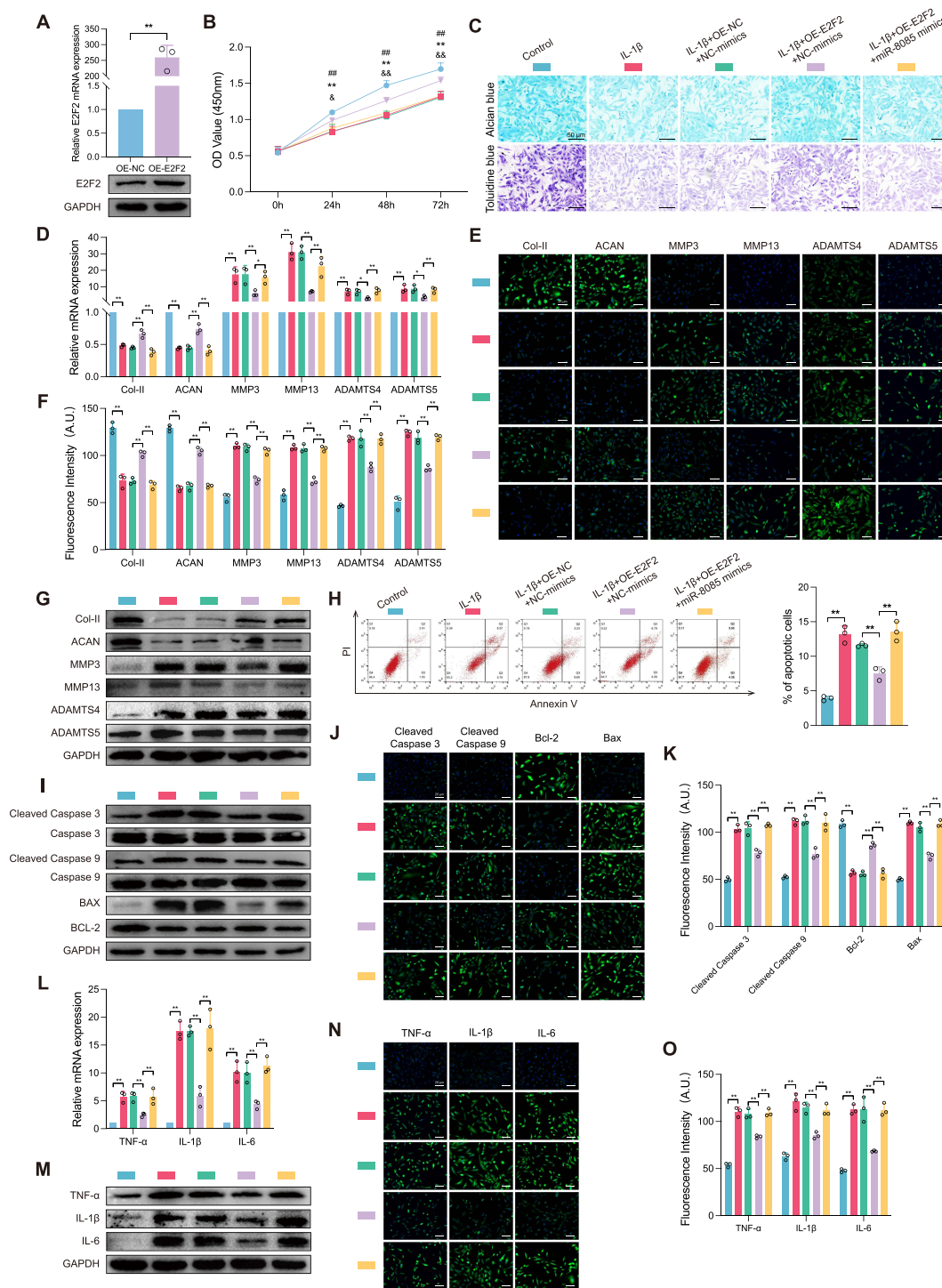
Figure 8 Lnc-PTS-1 regulated the miR-8085/E2F2 axis to protect against OA progression. (**A**) qRT-PCR and Western Blot analysis of E2F2 expression of C28/I2 cells transfected with overexpression plasmid or negative control (n=3). (**B**) CCK-8 assays were performed to determine the cell viability of miR-8085 mimics and E2F2 co-transfection with or without IL-1β at 24.48, and 72 h (**$P < 0.01$, Control vs IL-1β; ## $P < 0.01$, IL-1β+OE-NC+NC-mimics vs IL-1β+OE-E2F2+NC-mimics, & $P < 0.05$, && $P < 0.01$, IL-1β+OE-E2F2+NC-mimics vs IL-1β+OE-E2F2+miR-8085 mimics) (n=6). (**C**) Alcian blue and Toluidine blue staining (scale bar: 50 μm) were conducted to determine the ECM anabolism of E2F2 and miR-8085 mimics co-transfection with or without IL-1β (n=3). (**D**) qRT-PCR, (**E** and **F**) representative IF images (scale bar: 25 μm) and quantitative analysis, and (**G**) Western Blot analysis showed expression levels of ECM metabolism indicators of E2F2 and miR-8085 mimics co-transfected C28/I2 cells with or without IL-1β (n=3). (**H**) The apoptosis rate of C28/I2 cells was showed by flow cytometry (n=3). (**I**) Western Blot analysis, and (**J** and **K**) representative IF images (scale bar: 25 μm) and quantitative analysis showed apoptosis-related indicators expression of E2F2 and miR-8085 mimics co-transfected C28/I2 cells with or without IL-1β (n=3). (**L**) qRT-PCR, (**M**) Western Blot analysis, and (**N** and **O**) representative IF images (scale bar: 25 μm) and quantitative analysis showed expression levels of inflammatory factors of E2F2 and miR-8085 mimics co-transfected C28/I2 cells with or without IL-1β (n=3). Data are presented as mean ± SD, Statistical analysis was performed using unpaired t-tests (**A**) or one-way analysis of variance (ANOVA) (**B, D, F, H, K, L, O**); *$P < 0.05$, **$P < 0.01$.

and ACAN, key components of the cartilage ECM, compared to the Control group. Conversely, there was a significant upregulation in the expression of catabolic enzymes, including MMP3, MMP13, ADAMTS4, and ADAMTS5. Compared to the IL-1β+pcDNA+mimics-NC group, the IL-1β+OE-E2F2+mimics-NC group demonstrated a pronounced elevation in the ECM constituents' expression, alongside a suppression in ECM degradation. However, when E2F2 overexpression was accompanied by miR-8085 overexpression, C28/I2 cells exhibited an enhanced catabolism of the ECM (Figure 8D). Western Blot and IF staining have substantiated the protein expression profiles, validating the protective effects of E2F2 in countering IL-1β-induced chondrocyte degeneration, as well as delineating the suppressive impact of miR-8085 on E2F2 expression (Figure 8E-G).

To determine the role of E2F2 and miR-8085 in regulation of chondrocytes apoptosis, flow cytometry was used to detect the effects of E2F2 and miR-8085 overexpression on apoptosis and PI and annexin V double staining were done. The results showed that E2F2 could reduce the percentage of apoptosis cells whereas miR-8085 reversed this protective effect (Figure 8H). As illustrated by the results of Western Blot and IF staining, E2F2 overexpression mitigated the elevated expression of pro-apoptotic proteins (cleaved Caspase 3, cleaved Caspase 9, and Bax) induced by IL-1β, as well as the suppressive effect on the anti-apoptotic protein (BCL-2). However, miR-8085 abrogated the anti-apoptotic effects of E2F2 in chondrocytes (Figure 8I-K). Furthermore, our findings indicate that upregulation of E2F2 partially ameliorated the inflammatory response triggered by IL-1β, conversely, miR-8085 exacerbated the inflammatory response (Figure 8L-O).

Altogether, these results demonstrated that E2F2 mediated the effects of lnc-PTS-1/miR-8085 on ECM anabolism, anti-apoptosis and anti-inflammation in chondrocytes.

Discussion

Osteoarthritis (OA) is a leading cause of pain, limited mobility, and disability globally. Characterized by mechanical and biological dysfunction, OA is marked disturbances in the anabolic and catabolic metabolism of articular chondrocytes, ECM and subchondral bone. As the disease progresses, it can result in the loss of articular cartilage, subchondral bone sclerosis, bone destruction, osteophyte formation, and subchondral cyst development. Clinically, OA typically presents with pain, stiffness, functional limitations, and joint deformity.[33] The incidence and burden of OA are rising exponentially, with at least 240 million patients worldwide experiencing significant symptoms, including restricted joint movement.[34,35]

Although OA can be managed with both conservative and surgical treatments, these approaches only alleviate symptoms and slow the disease's progression without addressing its underlying etiology or pathology.[36] In recent years, as research on lncRNAs has expanded, numerous studies have demonstrated that lncRNAs play a significant role in regulating normal physiological processes and metabolism. They have also been shown to influence the development of various diseases as part of complex regulatory networks.[37,38] Increasing evidence indicates that lncRNAs exhibit differential expression during the onset and progression of OA and are involved in regulating cell proliferation, apoptosis, ECM synthesis and degradation, and inflammatory response in OA.[17,39–41] Therefore, by identifying OA-related lncRNAs and elucidating their mechanisms of action, it may be possible to develop new diagnostic biomarkers and therapeutic targets, offering new avenues for translating scientific research into clinical practice.

This study is the first to demonstrate that lnc-PTS-1 can target miR-8085 through "sponge binding", acting as a ceRNA to mitigate the inhibitory effect of miR-8085 on E2F2. By upregulating E2F2 expression, lnc-PTS-1 alleviates negative impacts on chondrocyte proliferation, ECM degradation, apoptosis, and inflammation, thereby delaying the progression of OA. Initially, we conducted high-throughput transcriptome sequencing on cartilage tissue samples from patients with OA and those without OA. From the lncRNAs with more than a 2-fold differential expression, we selected the top nine up-regulated and down-regulated lncRNAs for further investigation. We next used qRT-PCR to validate these findings in cartilage tissues from both OA patients and non-OA patients controls. Through this validation, combined with bioinformatics analysis, we identified lnc-PTS-1 as a candidate molecule for the subsequent study.

It is widely reported that IL-1β can be used to induce chondrocyte degeneration, creating an in vitro model of OA. Degenerating chondrocytes secrete IL-1β, which activates downstream gene expression, promoting key matrix-degrading

enzymes such as MMP3, MMP13, ADAMTS4, and ADAMTS5 to disrupt ECM homeostasis and further aggravate cell degeneration. Studies have shown that IL-1β-induced chondrocytes release increased levels of ADAMTS4 and ADAMTS5.[42] Additionally, IL-1β can induce apoptosis via the endogenous nitric oxide (NO) pathway. IL-1β stimulates chondrocytes to produce large amounts of NO, leading to apoptosis in vitro, whereas inhibiting NO synthase expression suppresses apoptosis and protects chondrocytes.[43] Furthermore, IL-1β increases the production of reactive oxygen species (ROS), leading to the formation of peroxides and hydroxyl radicals that directly damage articular cartilage.[44] A mouse OA model generated using IL-1β-induced chondrocyte apoptosis demonstrated that aucubin could protect articular cartilage in OA.[45] CircSERPINE2 was found to alleviate IL-1β-induced chondrocyte apoptosis and inflammation by targeting miR-1271 and ETS-related genes.[46] Given these findings, we selected IL-1β as the cytokine to establish a model of chondrocyte degeneration in vitro. By treating chondrocytes with varying concentrations of IL-1β, we measured indicators of cell proliferation, apoptosis, inflammation and ECM synthesis and degradation to validate the cell model's success and determine the optimal concentration for subsequent experiments. We observed that the expression of lnc-PTS-1 was downregulated in both IL-1β-treated C28/I2 cells and human primary chondrocytes, consistent with our sequencing data and tissue validation results.

To further clarify the relationship between lnc-PTS-1 and chondrocyte degeneration, plasmid and small interfering RNA (siRNA)-transfected cells were applied to modulate lnc-PTS-1 expression. The results indicated that downregulation of lnc-PTS-1 exacerbated IL-1β-induced chondrocyte degeneration, while upregulation of lnc-PTS-1 expression partially alleviated this effect. These findings suggest that lnc-PTS-1 plays a role in regulation IL-1β-induced chondrocyte degeneration.

What is the mechanism by which lnc-PTS-1 regulates chondrocyte degeneration? We discovered that lnc-PTS-1 is predominantly located in the cytoplasm, as shown by nuclear and cytoplasmic separation and fluorescence in situ hybridization experiments, suggesting that lnc-PTS-1 may act as a miRNA sponge, serving as a ceRNA to alleviate chondrocyte degeneration. Previous research has revealed that lncRNAs perform different biological functions depending on their cellular localization.[10] For example, LncRNA IGHCγ1 interacts with miR-6891-3p as a ceRNA to mediate TLR4/NF-κB expression, thereby accelerating the inflammatory response in chondrocytes.[47] Inspired by these findings, we explored whether lnc-PTS-1 might function through a ceRNA mechanism. We used siRNA to knock down lnc-PTS-1 expression, then combined this approach with miRNA differential expression profiles obtained through high-throughput miRNA sequencing analysis. Bioinformatics databases were used to predict downstream miRNA targets. Based on the RIP results and miRNA levels observed in the degeneration model in vitro, miR-8085 was identified as a downstream target for further functional verification. The dual luciferase reporter assays confirmed that lnc-PTS-1 can directly target and bind miR-8085. Additionally, in vitro functional experiments revealed that upregulating miR-8085 expression could counteract the effects of lnc-PTS-1 overexpression on IL-1β-induced chondrocyte proliferation inhibition, ECM degradation, apoptosis, and inflammation. These above findings illustrate that lnc-PTS-1 functions as ceRNA by binding to miRNA-8085, thereby participating in the regulation of chondrocyte degeneration.

It is well established that miRNAs perform their biological functions by regulating the translation of their downstream target genes. miRNAs can bind to the 3' UTR region of target mRNAs with full or partial complementarity, leading to mRNA cleavage, blocking the translation process, and ultimately inhibiting protein synthesis.[48] A growing body of research has demonstrated that miRNAs play a crucial role in maintaining microenvironmental homeostasis in OA.[49] For instance, overexpression of miR-34a promotes chondrocyte senescence and apoptosis by targeting the Notch signaling pathway.[50] Conversely, knocking down miR-34a expression reduces IL-1β-induced apoptosis in rat chondrocytes.[51] MiR-335-5p is expressed at lower levels in OA than in normal chondrocytes, and its overexpression can enhance autophagy and suppress inflammation.[52] Additionally, miR-495 is highly expressed in human OA cartilage, and its overexpression directly targets the AKT/mTOR signaling pathway, upregulates senescence markers (SA-β-gal and p16), and contributes to chondrocyte apoptosis.[53] To identify the downstream target genes of miR-8085 and their role in chondrocyte degeneration, we constructed and analyzed differential mRNA expression profiles between lnc-PTS-1 down-regulated and control groups. Using bioinformatics tools such as RNAhybrid, Miranda, and TargetScan for miRNA target gene prediction, we identified E2F2 as a potential candidate target for further validation.

We further demonstrated that E2F2 directly binds to and is targeted by miR-8085, as shown by a dual luciferase reporter assay. Our findings revealed a negative correlation between the expression of lnc-PTS-1 and E2F2 with miR-8085 in degenerating chondrocytes. Modulating the levels of lnc-PTS-1 and miR-8085 influenced the expression of E2F2 at both the gene and protein levels. Specifically, lnc-PTS-1 acts as a ceRNA by "sponge binding" miR-8085, thereby indirectly regulating the expression of E2F2 mRNA and protein. Moreover, overexpression of lnc-PTS-1 partially mitigated the detrimental effects of IL-1β on chondrocyte proliferation, apoptosis, inflammatory response, and ECM degradation by indirectly upregulating E2F2 expression. This protective effect was reversed when miR-8085 was overexpressed. Our data above suggested that lnc-PTS-1 alleviated IL-1β-induced chondrocyte degeneration by upregulating E2F2 through its interaction with miR-8085.

Conclusion

In summary, our study identified a significant number of differentially expressed lncRNAs in cartilage tissues of patients with OA compared to those without OA, highlighting that lnc-PTS-1 was downregulated in both OA patients and cellular models in vitro. The downregulation of lnc-PTS-1 further exacerbated IL-1β-induced chondrocyte degeneration, whereas its upregulation alleviated these adverse effects through the miR-8085/E2F2 axis. This study not only elucidated the specific role of lnc-PTS-1 in regulating chondrocyte proliferation, apoptosis, inflammation, and ECM metabolism, but also revealed the cellular and molecular mechanism by which lnc-PTS-1 regulated E2F2 via miR-8085, contributing to OA progression. These findings provide theoretical basis and experimental evidence for the potential clinical application of new LncRNA molecules in the treatment of OA.

Acknowledgments

Disclosure

The authors report no conflicts of interest in this work.

References

1. Hunter DJ, March L, Chew M. Osteoarthritis in 2020 and beyond: a lancet commission. *Lancet*. 2020;396(10264):1711–1712. doi:10.1016/S0140-6736(20)32230-3
2. Georgiev T, Angelov AK. Modifiable risk factors in knee osteoarthritis: treatment implications. *Rheumatol Int*. 2019;39(7):1145–1157. doi:10.1007/s00296-019-04290-z
3. O'Neill TW, McCabe PS, McBeth J. Update on the epidemiology, risk factors and disease outcomes of osteoarthritis. *Best Pract Res Clin Rheumatol*. 2018;32(2):312–326. doi:10.1016/j.berh.2018.10.007
4. Mobasheri A, Batt M. An update on the pathophysiology of osteoarthritis. *Ann Phys Rehabil Med*. 2016;59(5–6):333–339. doi:10.1016/j.rehab.2016.07.004
5. Musumeci G, Aiello FC, Szychlinska MA, Di Rosa M, Castrogiovanni P, Mobasheri A. Osteoarthritis in the XXIst century: risk factors and behaviours that influence disease onset and progression. *Int J Mol Sci*. 2015;16(3):6093–6112. doi:10.3390/ijms16036093
6. Goldring MB, Goldring SR. Articular cartilage and subchondral bone in the pathogenesis of osteoarthritis. *Ann N Y Acad Sci*. 2010;1192(1):230–237. doi:10.1111/j.1749-6632.2009.05240.x
7. Mort JS, Billington CJ. Articular cartilage and changes in arthritis: matrix degradation. *Arthritis Res*. 2001;3(6):337–341. doi:10.1186/ar325
8. Abramoff B, Caldera FE. Osteoarthritis: pathology, diagnosis, and treatment options. *Med Clin North Am*. 2020;104(2):293–311. doi:10.1016/j.mcna.2019.10.007
9. Postler A, Lutzner C, Beyer F, Tille E, Lutzner J. Analysis of total knee arthroplasty revision causes. *BMC Musculoskelet Disord*. 2018;19(1):55. doi:10.1186/s12891-018-1977-y
10. Bridges MC, Daulagala AC, Kourtidis A. LNCcation: lncRNA localization and function. *J Cell Biol*. 2021;220(2). doi:10.1083/jcb.202009045
11. Zuckerman B, Ron M, Mikl M, Segal E, Ulitsky I. Gene architecture and sequence composition underpin selective dependency of nuclear export of long RNAs on NXF1 and the TREX complex. *Mol Cell*. 2020;79(2):251–267e6. doi:10.1016/j.molcel.2020.05.013
12. Mukherjee N, Calviello L, Hirsekorn A, de Pretis S, Pelizzola M, Ohler U. Integrative classification of human coding and noncoding genes through RNA metabolism profiles. *Nat Struct Mol Biol*. 2017;24(1):86–96. doi:10.1038/nsmb.3325
13. Cabili MN, Dunagin MC, McClanahan PD, et al. Localization and abundance analysis of human lncRNAs at single-cell and single-molecule resolution. *Genome Biol*. 2015;16(1):20. doi:10.1186/s13059-015-0586-4

14. Zhang X, Liu Q, Zhang J, et al. The emerging role of lncRNAs in osteoarthritis development and potential therapy. *Front Genet*. 2023;14:1273933. doi:10.3389/fgene.2023.1273933

15. Abbasifard M, Kamiab Z, Bagheri-Hosseinabadi Z, Sadeghi I. The role and function of long non-coding RNAs in osteoarthritis. *Exp Mol Pathol*. 2020;114:104407. doi:10.1016/j.yexmp.2020.104407

16. Wang Y, Li T, Yang Q, et al. LncRNA THUMPD3-AS1 enhances the proliferation and inflammatory response of chondrocytes in osteoarthritis. *Int Immunopharmacol*. 2021;100:108138. doi:10.1016/j.intimp.2021.108138

17. Tian F, Wang J, Zhang Z, Yang J. LncRNA SNHG7/miR-34a-5p/SYVN1 axis plays a vital role in proliferation, apoptosis and autophagy in osteoarthritis. *Biol Res*. 2020;53(1):9. doi:10.1186/s40659-020-00275-6

18. Cao L, Wang Y, Wang Q, Huang J. LncRNA FOXD2-AS1 regulates chondrocyte proliferation in osteoarthritis by acting as a sponge of miR-206 to modulate CCND1 expression. *Biomed Pharmacother*. 2018;106:1220–1226. doi:10.1016/j.biopha.2018.07.048

19. Zhao Y, Zhao J, Guo X, She J, Liu Y. Long non-coding RNA PVT1, a molecular sponge for miR-149, contributes aberrant metabolic dysfunction and inflammation in IL-1beta-simulated osteoarthritic chondrocytes. *Biosci Rep*. 2018;38(5). doi:10.1042/BSR20180576

20. Vincent TL. IL-1 in osteoarthritis: time for a critical review of the literature. *F1000Res*. 2019;8:934. doi:10.12688/f1000research.18831.1

21. Attur M, Krasnokutsky S, Statnikov A, et al. Low-grade inflammation in symptomatic knee osteoarthritis: prognostic value of inflammatory plasma lipids and peripheral blood leukocyte biomarkers. *Arthritis Rheumatol*. 2015;67(11):2905–2915. doi:10.1002/art.39279

22. Sun H, Peng G, Ning X, Wang J, Yang H, Deng J. Emerging roles of long noncoding RNA in chondrogenesis, osteogenesis, and osteoarthritis. *Am J Transl Res*. 2019;11(1):16–30.

23. Chen WK, Yu XH, Yang W, et al. lncRNAs: novel players in intervertebral disc degeneration and osteoarthritis. *Cell Prolif*. 2017;50(1). doi:10.1111/cpr.12313

24. Li Q, Zhang Z, Guo S, Tang G, Lu W, Qi X. LncRNA ANCR is positively correlated with transforming growth factor-beta1 in patients with osteoarthritis. *J Cell Biochem*. 2019;120(9):14226–14232. doi:10.1002/jcb.28881

25. Diener C, Keller A, Meese E. Emerging concepts of miRNA therapeutics: from cells to clinic. *Trends Genet*. 2022;38(6):613–626. doi:10.1016/j.tig.2022.02.006

26. Malemud CJ. MicroRNAs and Osteoarthritis. *Cells*. 2018;7(8):92. doi:10.3390/cells7080092

27. Ciuffi S, Marini F, Fossi C, et al. Circulating MicroRNAs as biomarkers of osteoporosis and fragility fractures. *J Clin Endocrinol Metab*. 2022;107(8):2267–2285. doi:10.1210/clinem/dgac293

28. Laresgoiti U, Apraiz A, Olea M, et al. E2F2 and CREB cooperatively regulate transcriptional activity of cell cycle genes. *Nucleic Acids Res*. 2013;41(22):10185–10198. doi:10.1093/nar/gkt821

29. Gao Y, Qiao X, Liu Z, Zhang W. The role of E2F2 in cancer progression and its value as a therapeutic target. *Front Immunol*. 2024;15:1397303. doi:10.3389/fimmu.2024.1397303

30. Wang S, Wang L, Wu C, Sun S, Pan JH. E2F2 directly regulates the STAT1 and PI3K/AKT/NF-kappaB pathways to exacerbate the inflammatory phenotype in rheumatoid arthritis synovial fibroblasts and mouse embryonic fibroblasts. *Arthritis Res Ther*. 2018;20(1):225. doi:10.1186/s13075-018-1713-x

31. Ma C, Qi X, Wei YF, et al. Amelioration of ligamentum flavum hypertrophy using umbilical cord mesenchymal stromal cell-derived extracellular vesicles. *Bioact Mater*. 2023;19:139–154. doi:10.1016/j.bioactmat.2022.03.042

32. Ma C, Liu H, Wei Y, Li H, Miao D, Ren Y. Exogenous PTH 1-34 attenuates impaired fracture healing in endogenous PTH deficiency mice via activating Indian hedgehog signaling pathway and accelerating endochondral ossification. *Front Cell Dev Biol*. 2021;9:750878. doi:10.3389/fcell.2021.750878

33. Mandl LA. Osteoarthritis year in review 2018: clinical. *Osteoarthritis Cartilage*. 2019;27(3):359–364. doi:10.1016/j.joca.2018.11.001

34. Global Burden of Disease Study C. Global, regional, and national incidence, prevalence, and years lived with disability for 301 acute and chronic diseases and injuries in 188 countries, 1990-2013: a systematic analysis for the global burden of disease study 2013. *Lancet*. 2015;386(9995):743–800. doi:10.1016/S0140-6736(15)60692-4

35. Hunter DJ, Schofield D, Callander E. The individual and socioeconomic impact of osteoarthritis. *Nat Rev Rheumatol*. 2014;10(7):437–441. doi:10.1038/nrrheum.2014.44

36. Katz JN, Arant KR, Loeser RF. Diagnosis and treatment of hip and knee osteoarthritis: a review. *JAMA*. 2021;325(6):568–578. doi:10.1001/jama.2020.22171

37. Li D, Yang C, Yin C, et al. LncRNA, important player in bone development and disease. *Endocr Metab Immune Disord Drug Targets*. 2020;20(1):50–66. doi:10.2174/1871530319666190904161707

38. Schmitz SU, Grote P, Herrmann BG. Mechanisms of long noncoding RNA function in development and disease. *Cell Mol Life Sci*. 2016;73(13):2491–2509. doi:10.1007/s00018-016-2174-5

39. Zhang Y, Wang F, Chen G, He R, Yang L. LncRNA MALAT1 promotes osteoarthritis by modulating miR-150-5p/AKT3 axis. *Cell Biosci*. 2019;9(1):54. doi:10.1186/s13578-019-0302-2

40. Xiao Y, Yan X, Yang Y, Ma X. Downregulation of long noncoding RNA HOTAIRM1 variant 1 contributes to osteoarthritis via regulating miR-125b/BMPR2 axis and activating JNK/MAPK/ERK pathway. *Biomed Pharmacother*. 2019;109:1569–1577. doi:10.1016/j.biopha.2018.10.181

41. Wang A, Hu N, Zhang Y, et al. MEG3 promotes proliferation and inhibits apoptosis in osteoarthritis chondrocytes by miR-361-5p/FOXO1 axis. *BMC Med Genomics*. 2019;12(1):201. doi:10.1186/s12920-019-0649-6

42. Guo D, Ding L, Homandberg GA. Telopeptides of type II collagen upregulate proteinases and damage cartilage but are less effective than highly active fibronectin fragments. *Inflamm Res*. 2009;58(3):161–169. doi:10.1007/s00011-009-8090-5

43. Leonidou A, Lepetsos P, Mintzas M, et al. Inducible nitric oxide synthase as a target for osteoarthritis treatment. *Expert Opin Ther Targets*. 2018;22(4):299–318. doi:10.1080/14728222.2018.1448062

44. Chen Z, Zhong H, Wei J, et al. Inhibition of Nrf2/HO-1 signaling leads to increased activation of the NLRP3 inflammasome in osteoarthritis. *Arthritis Res Ther*. 2019;21(1):300. doi:10.1186/s13075-019-2085-6

45. Wang BW, Jiang Y, Yao ZL, Chen PS, Yu B, Wang SN. Aucubin protects chondrocytes against IL-1beta-induced apoptosis in vitro and inhibits osteoarthritis in mice model. *Drug Des Devel Ther*. 2019;13:3529–3538. doi:10.2147/DDDT.S210220

46. Shen S, Wu Y, Chen J, et al. CircSERPINE2 protects against osteoarthritis by targeting miR-1271 and ETS-related gene. *Ann Rheum Dis*. 2019;78(6):826–836. doi:10.1136/annrheumdis-2018-214786

47. Zhang P, Sun J, Liang C, et al. lncRNA IGHCgamma1 Acts as a ceRNA to regulate macrophage inflammation via the miR-6891-3p/TLR4 axis in osteoarthritis. *Mediators Inflamm*. 2020;2020:9743037. doi:10.1155/2020/9743037

48. Liu B, Li J, Cairns MJ. Identifying miRNAs, targets and functions. *Brief Bioinform*. 2014;15(1):1–19. doi:10.1093/bib/bbs075

49. Swingler TE, Niu L, Smith P, et al. The function of microRNAs in cartilage and osteoarthritis. *Clin Exp Rheumatol*. 2019;37 Suppl 120(5):40–47.

50. Zhang W, Hsu P, Zhong B, et al. MiR-34a enhances chondrocyte apoptosis, senescence and facilitates development of osteoarthritis by targeting DLL1 and regulating PI3K/AKT pathway. *Cell Physiol Biochem*. 2018;48(3):1304–1316. doi:10.1159/000492090

51. Abouheif MM, Nakasa T, Shibuya H, Niimoto T, Kongcharoensombat W, Ochi M. Silencing microRNA-34a inhibits chondrocyte apoptosis in a rat osteoarthritis model in vitro. *Rheumatology*. 2010;49(11):2054–2060. doi:10.1093/rheumatology/keq247

52. Zhong G, Long H, Ma S, Shunhan Y, Li J, Yao J. miRNA-335-5p relieves chondrocyte inflammation by activating autophagy in osteoarthritis. *Life Sci*. 2019;226:164–172. doi:10.1016/j.lfs.2019.03.071

53. Zhao X, Wang T, Cai B, et al. MicroRNA-495 enhances chondrocyte apoptosis, senescence and promotes the progression of osteoarthritis by targeting AKT1. *Am J Transl Res*. 2019;11(4):2232–2244.